B-Mode Image Recovery with Aperture Domain Model Image Reconstruction (ADMIRE)

Brett Byram

BIOMEDICAL ELASTICITY & ACOUSTIC MEASUREMENT LAB

AAPM 2017

Explicit Models for Ultrasound Image Formation

$$y = X\beta$$

⋮

Byram and Jakovljevic. IEEE UFFC, 2014.
Byram et al. IEEE UFFC, 2015.
Szasz et al. IEEE UFFC, 2016.
Guillaume et al., IEEE IUS, 2016.
Shin and Huang, IEEE TMI, 2017.

⋮

Explicit Models for Ultrasound Image Formation

$$y = X\beta$$

Need to determine how to solve for this.

Need to determine what goes here.

⋮

Byram and Jakovljevic. IEEE UFFC, 2014.
Byram et al. IEEE UFFC, 2015.
Szasz et al. IEEE UFFC, 2016.
Guillaume et al., IEEE IUS, 2016.
Shin and Huang, IEEE TMI, 2017.

⋮

Occasionally "Glass-Walled" patients are encountered clinically...

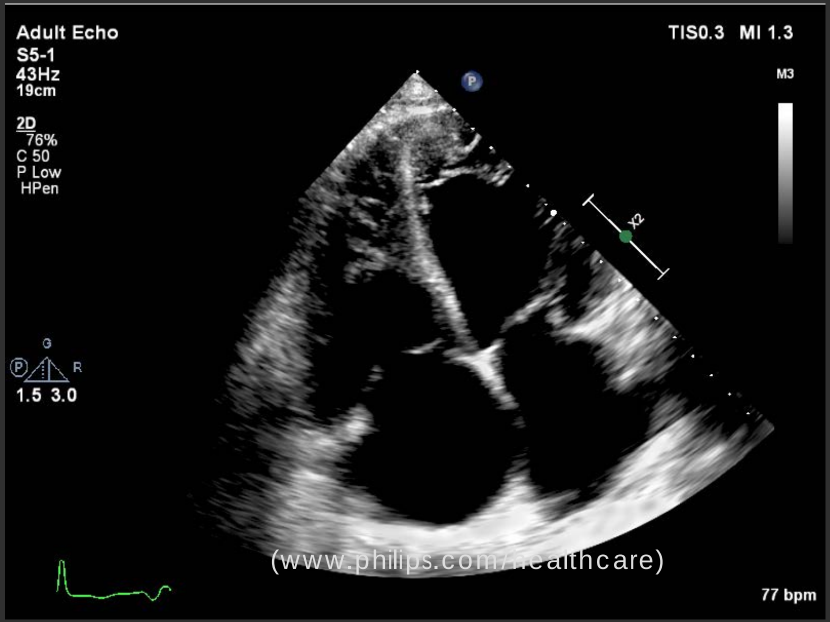

(www.philips.com/healthcare)

In Normal Patient Populations Ultrasound is Hard!

Occasionally "Glass-Walled" patients are encountered clinically...

...Typically quality is more mediocre.

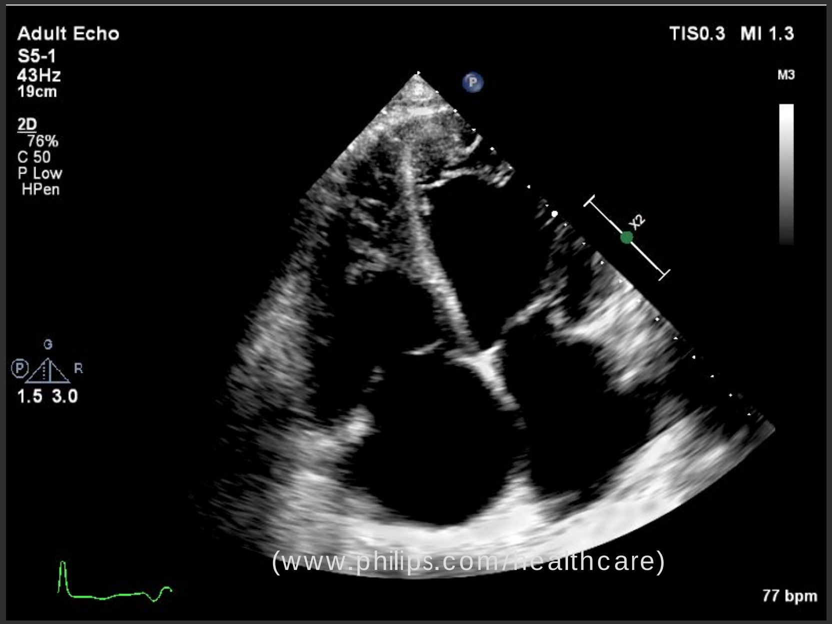

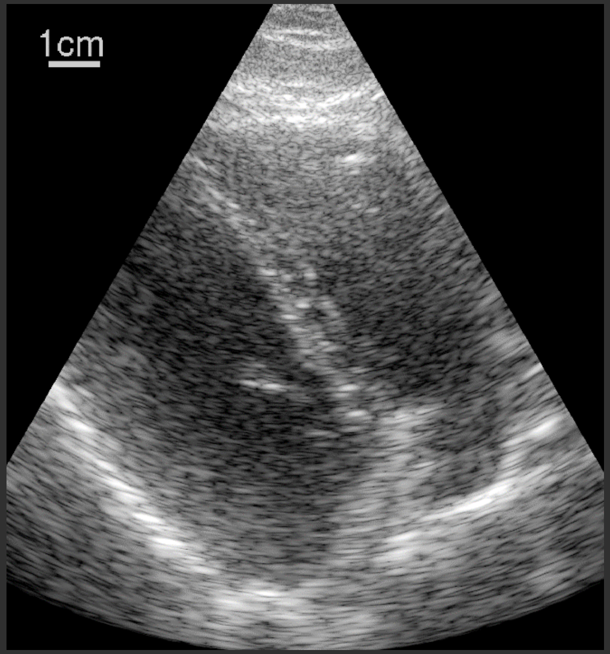

In Normal Patient Populations Ultrasound is Hard!

Occasionally "Glass-Walled" patients are encountered clinically...

...Typically quality is more mediocre.

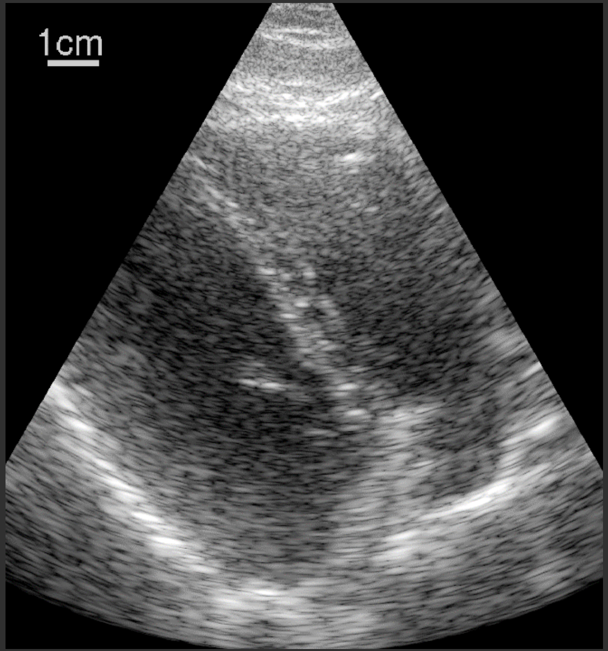

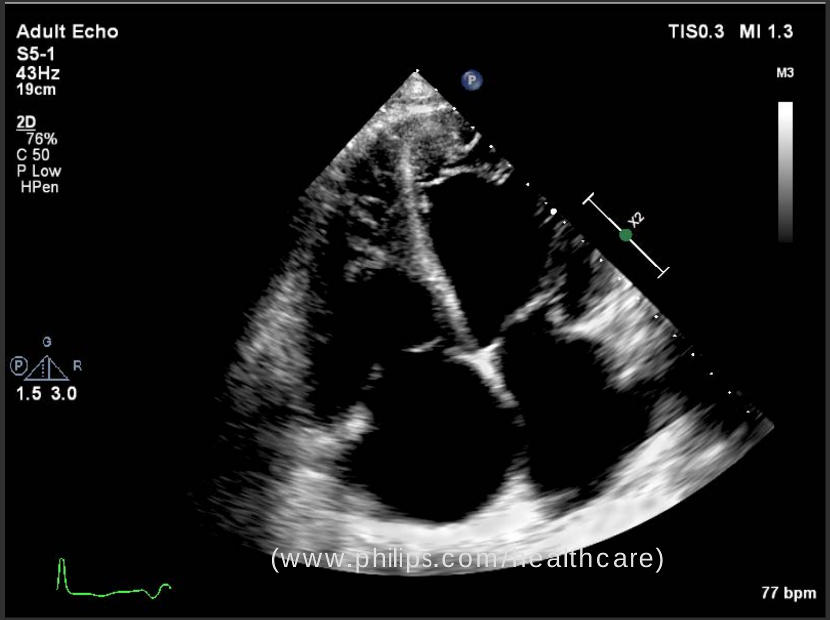

(www.philips.com/healthcare)

Clinical Failure Rates:

Obstetrics[4-7]	11-64%
Cardiac TTE[1-3]	9-64%

TTE inadequate[8]	98.4%

[1] Flynn et al. *Jrnl. of cardiothoracic and vascular anesthesia*, 2010.
[2] Garrett et al. *Annals of vascular surgery*, 2004.
[3] Heidenreich. *Jrnl. of the American College of Cardiology*, 1995.
[4] Hendler et al. *Jrnl of the Intl. Ass. for the Study of Obesity*, 2004.
[5] Hendler et al. *Journal of ultrasound in medicine*, 2005.
[6] Hendler et al. *American journal of obstetrics and gynecology*, 2004.
[7] Khoury et al. *The journal of maternal-fetal & neonatal medicine*, 2009.
[8] Kurt et al., *Journal of the American College of Cardiology*, 2009.

In Normal Patient Populations Ultrasound is Hard!

Why does ultrasound fail?

~~Why does ultrasound fail?~~

Why do ultrasound exams have such a wide variability in outcome?

- Pressure wave attenuation [1]
- Diffraction-limitations [2,3]
- Multiple scattering or reverberation (sometimes considered distinct) [2, 4, 5],
- Gross sound-speed deviation[6]
- Sound speed and attenuation inhomogeneities [7–13]

[1] Douglas Christensen. *Ultrasonic Bioinstrumentation*. John Wiley and Sons, New York, 1988.

[2] P L Carson and T V Oughton. A modeled study for diagnosis of small anechoic masses with ultrasound. *Radiology*, 122(3):765–71, March 1977.

[3] L. E. Hann, A. M. Bach, L. D. Cramer, D. Siegel, H. H. Yoo, and R. Garcia. Hepatic sonography: comparison of tissue harmonic and standard sonography techniques. *AJR. American journal of roentgenology*, 173(1):201–206, Jul 1999.

[4] S H P Bly, F S Foster, M S Patterson, D R Foster, and J W Hunt. Artifactual Echoes in B-Mode Images due to Multiple Scattering. *Ultrasound Med. Biol.*, 11(1):99–111, 1985.

[5] Gianmarco F Pinton, Gregg E Trahey, and Jeremy J Dahl. Erratum: Sources of image degradation in fundamental and harmonic ultrasound imaging: a nonlinear, full-wave, simulation study. *Ultrasonics, Ferroelectrics and Frequency Control, IEEE Transactions on*, 58(6):1272–83, June 2011.

[6] Martin E Anderson and Gregg E Trahey. The direct estimation of sound speed using pulse-echo ultrasound. *J. Acoust. Soc. Am.*, 104(5):3099–3106, November 1998.

[7] S.W. Smith, G.E. Trahey, and O.T. von Ramm. Phased array ultrasound imaging through planar tissue layers. *Ultrasound Med. Biol.*, 12(3):229 – 243, 1986.

[8] L. M. Hinkelman, D. L. Liu, L. A. Metlay, and R. C. Waag. Measurements of ultrasonic pulse arrival time and energy level variations produced by propagation through abdominal wall. *J. Acoust. Soc. Am.*, 95(1):530–541, Jan 1994.

[9] Makoto Tabei, T Douglas Mast, and Robert C Waag. Simulation of ultrasonic focus aberration and correction through human tissue. *J. Acoust. Soc. Am.*, 113(2):1166–76, 2003.

[10] S W Flax and M O'Donnell. Phase-aberration correction using signals from point reflectors and diffuse scatterers: basic principles. *Ultrasonics, Ferroelectrics and Frequency Control, IEEE Transactions on*, 35(6):758–67, January 1988.

[11] Q. Zhu and B. D. Steinberg. Large-transducer measurements of wavefront distortion in the female breast. *Ultrasonic imaging*, 14(3):276–299, Jul 1992.

[12] Y. Sumino and R. C. Waag. Measurements of ultrasonic pulse arrival time differences produced by abdominal wall specimens. *J. Acoust. Soc. Am.*, 90(6):2924–2930, Dec 1991.

[13] R.C. Waag, J.P. Astheimer, and Jr. Swartout, G. W. A characterization of wavefront distortion for analysis of ultrasound diffraction measurements made through an nhomogeneous medium. *Sonics and Ultrasonics, IEEE Transactions on*, 32(1):36–48, Jan 1985.

Sources of Image Degradation

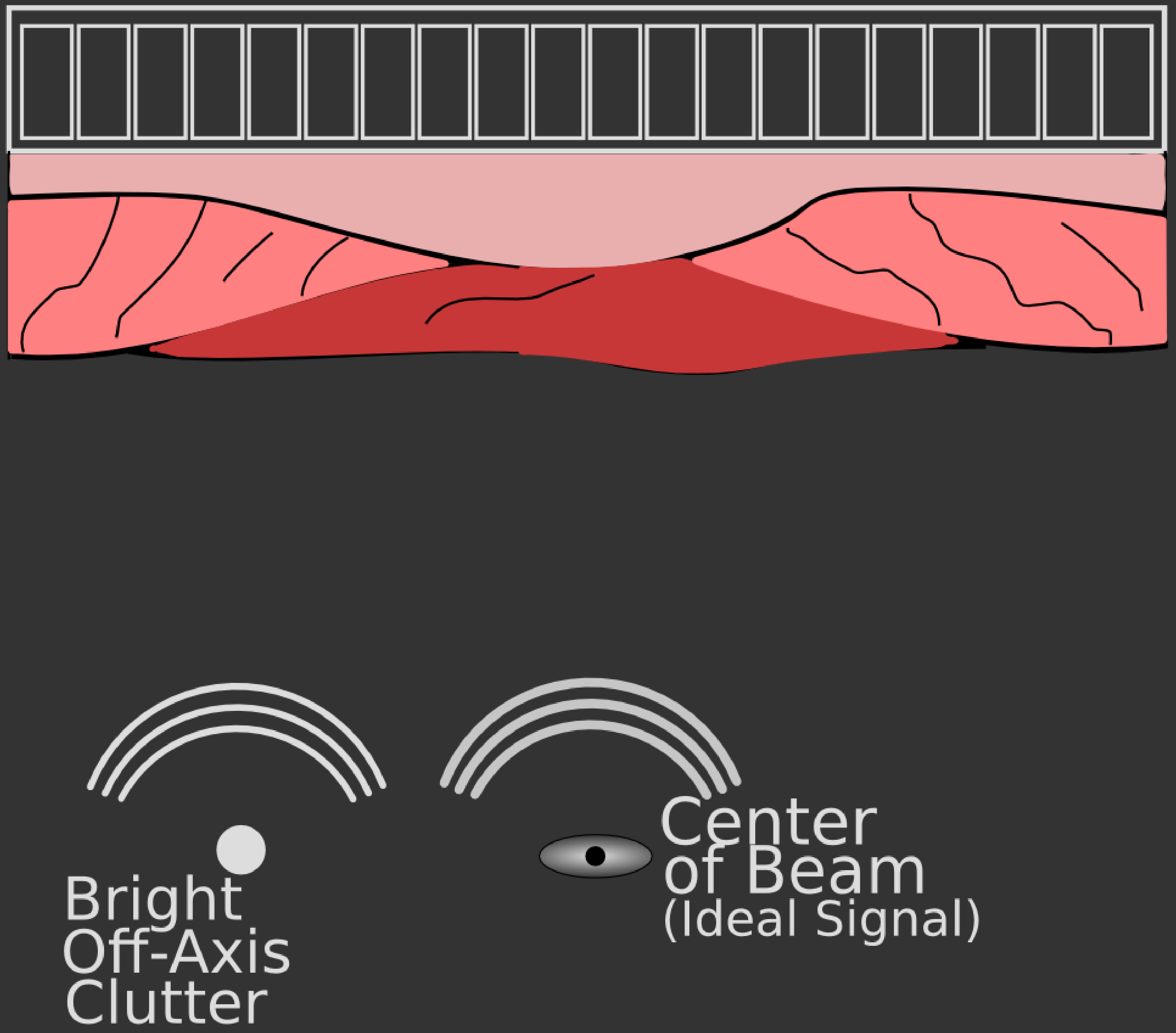

Bright Off-Axis Scattering

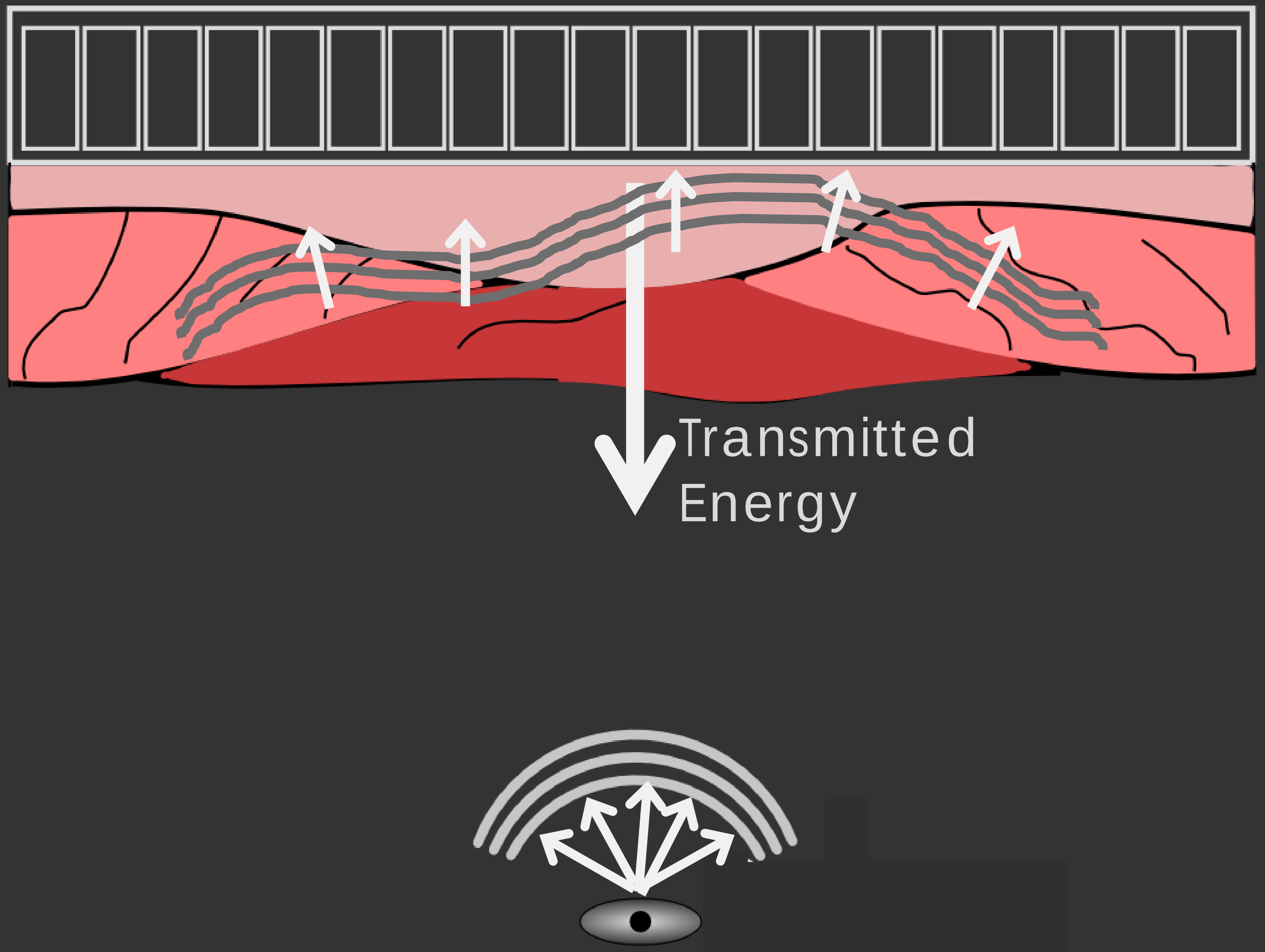

Wavefront Distortion (Phase Aberration)

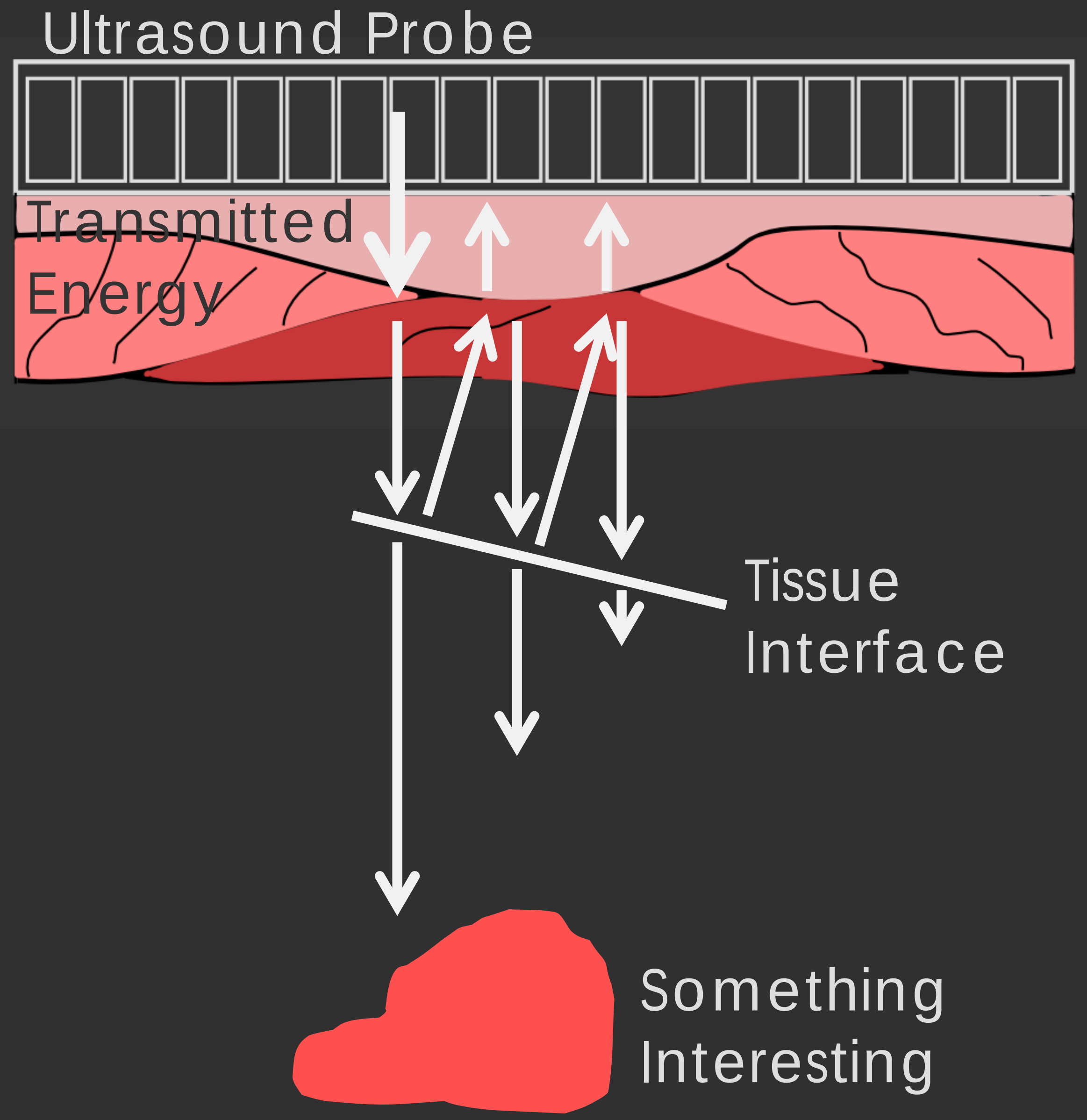

Reverberation (Multipath Scattering)

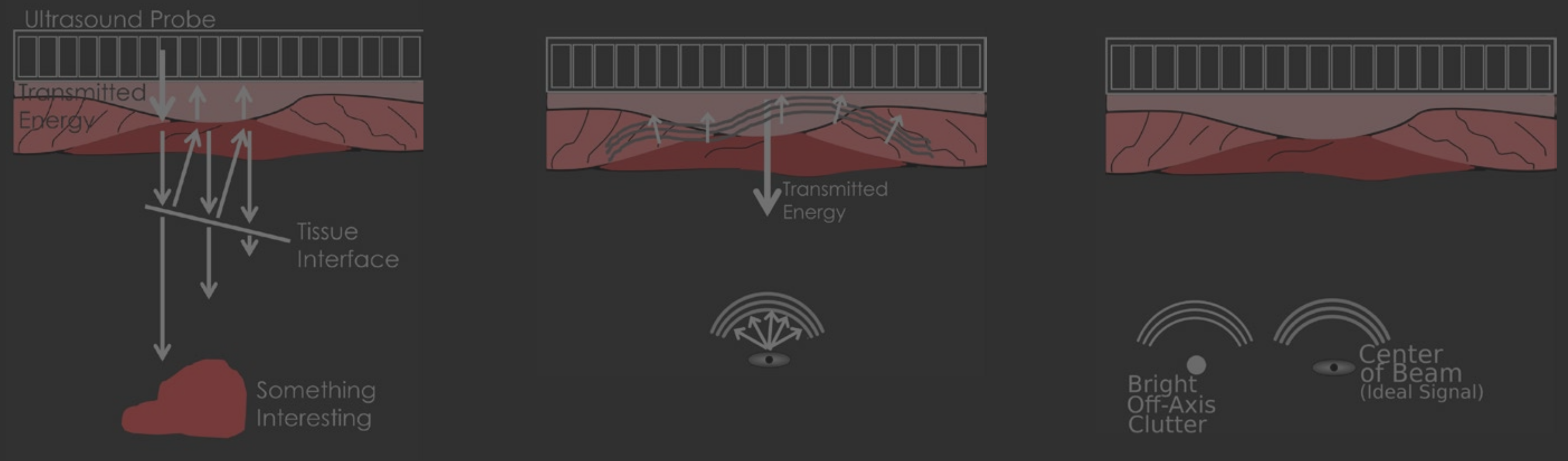

What about resolution?

Aperture **D**omain **M**odel **I**mage **RE**construction (ADMIRE)

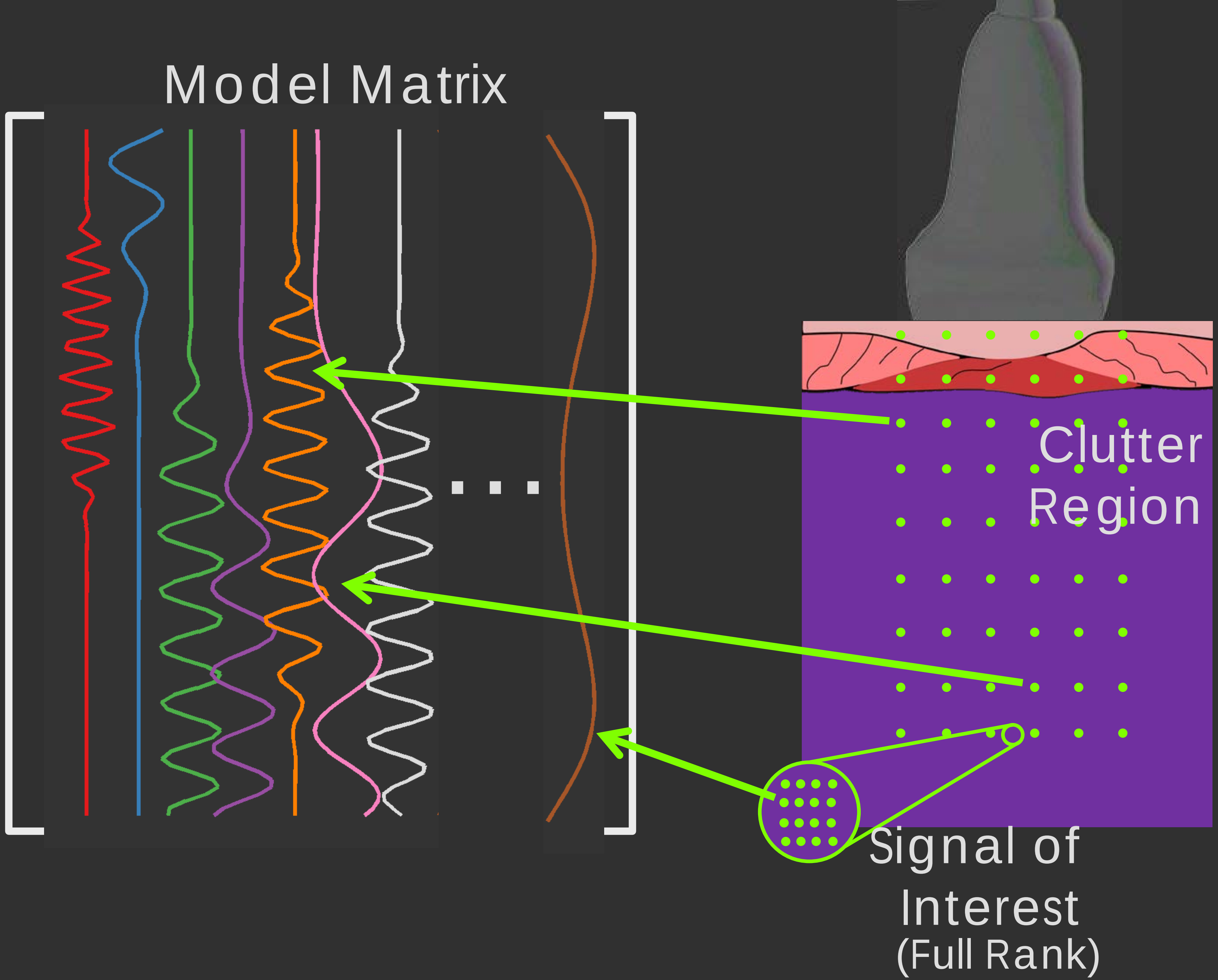
Model Matrix
Clutter Region
Signal of Interest
(Full Rank)

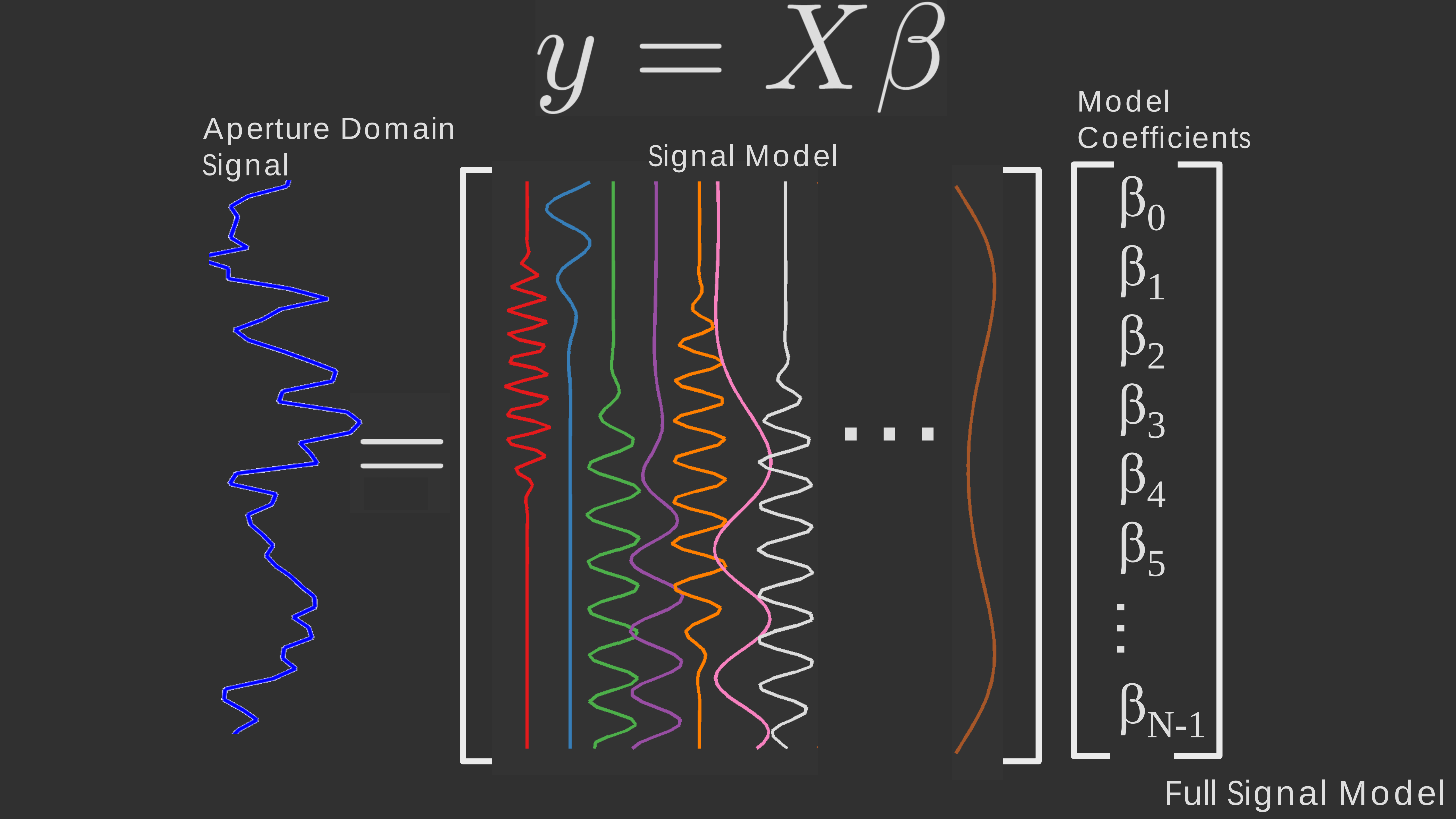
$y = X\beta$
Aperture Domain Signal
Signal Model
Model Coefficients
β_0
β_1
β_2
β_3
β_4
β_5
β_{N-1}
Full Signal Model

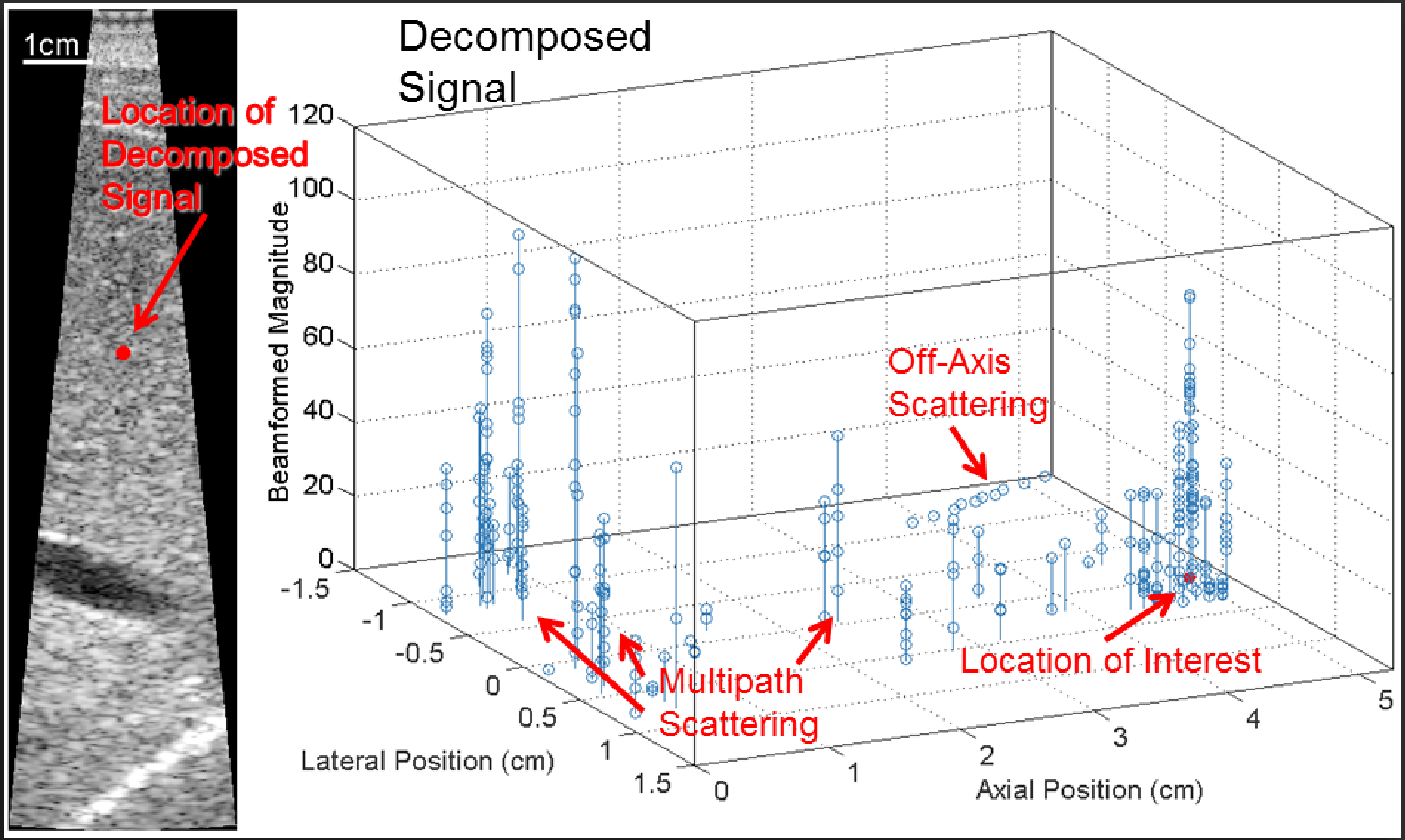

Model Identifies Spatial Distribution of Energy → Reconstruct the Energy of Interest

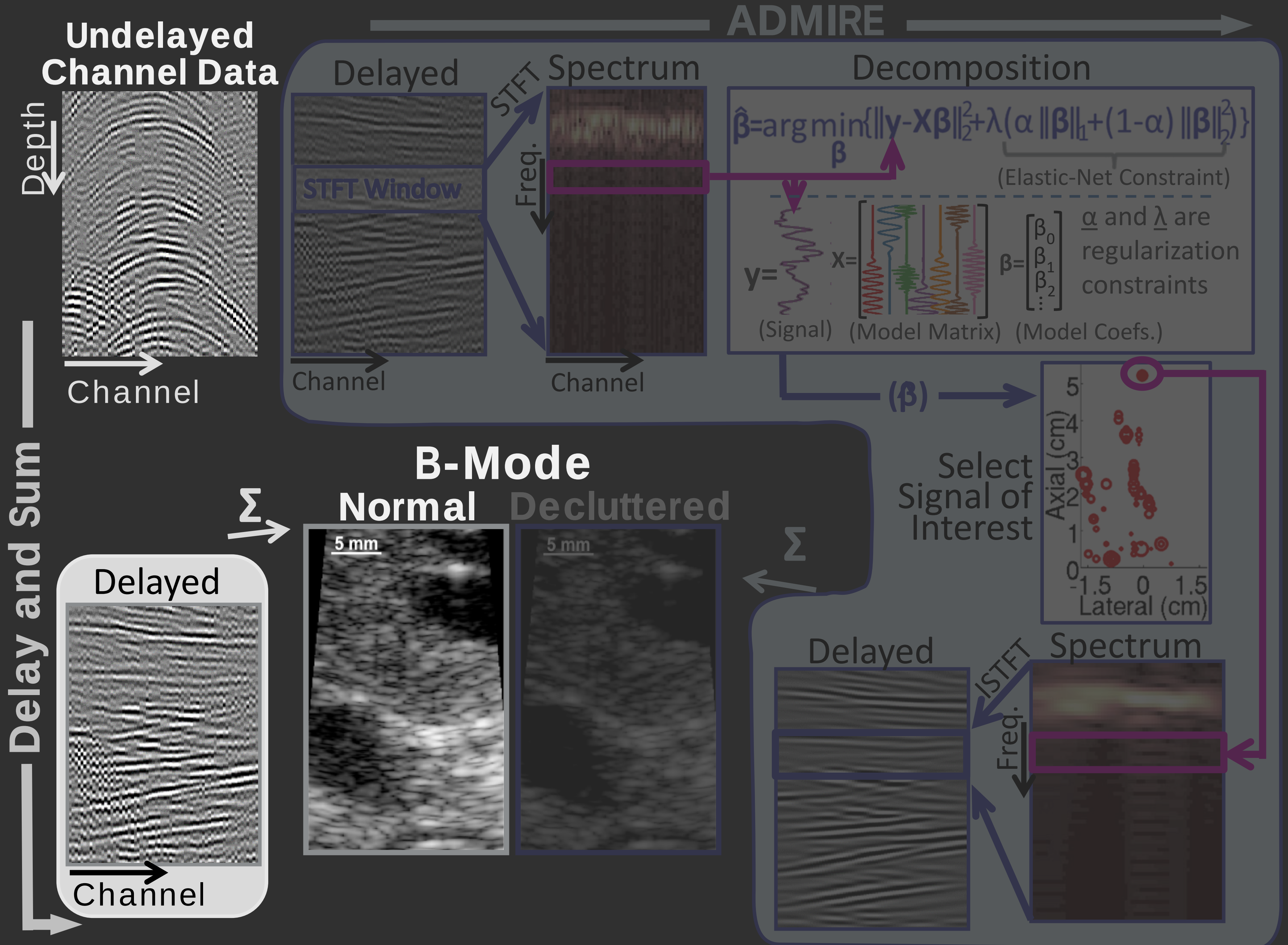

ADMIRE
Undelayed Channel Data
Depth
Channel
Delayed
STFT Window
Channel
STFT
Spectrum
Freq.
Channel
Decomposition
$\hat{\beta}=\arg\min_{\beta}\{\|y-X\beta\|_2^2+\lambda(\alpha\|\beta\|_1+(1-\alpha)\|\beta\|_2^2)\}$
(Elastic-Net Constraint)
y=
X=
β=
(Signal)
(Model Matrix)
(Model Coefs.)
α and λ are regularization constraints
(β)
Select Signal of Interest
Axial (cm)
Lateral (cm)
Delayed
ISTFT
Spectrum
Freq.
Σ
B-Mode
Normal
Decluttered
5 mm
5 mm
Σ
Delay and Sum
Delayed
Channel

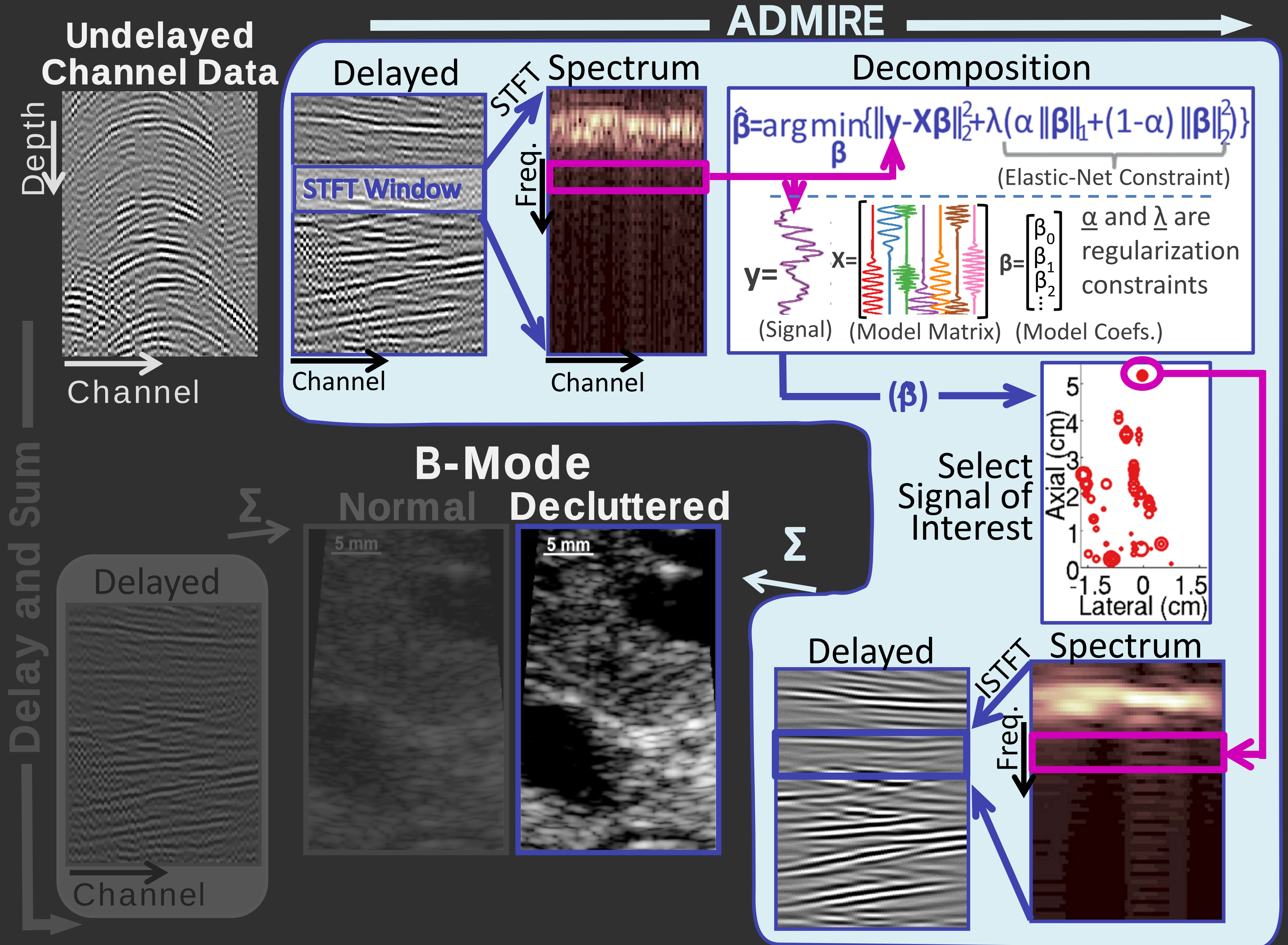

ADMIRE
Undelayed Channel Data
Depth
Channel
Delayed
STFT Window
Channel
STFT
Spectrum
Freq.
Channel
Decomposition
$\hat{\beta}=\arg\min_{\beta}\{\|y-X\beta\|_2^2+\lambda(\alpha\|\beta\|_1+(1-\alpha)\|\beta\|_2^2)\}$
(Elastic-Net Constraint)
y=
X=
β=
α and λ are regularization constraints
(Signal)
(Model Matrix)
(Model Coefs.)
(β)
Select Signal of Interest
Axial (cm)
Lateral (cm)
Delay and Sum
Delayed
Channel
B-Mode
Normal
Decluttered
5 mm
5 mm
Σ
Σ
Delayed
ISTFT
Spectrum
Freq.

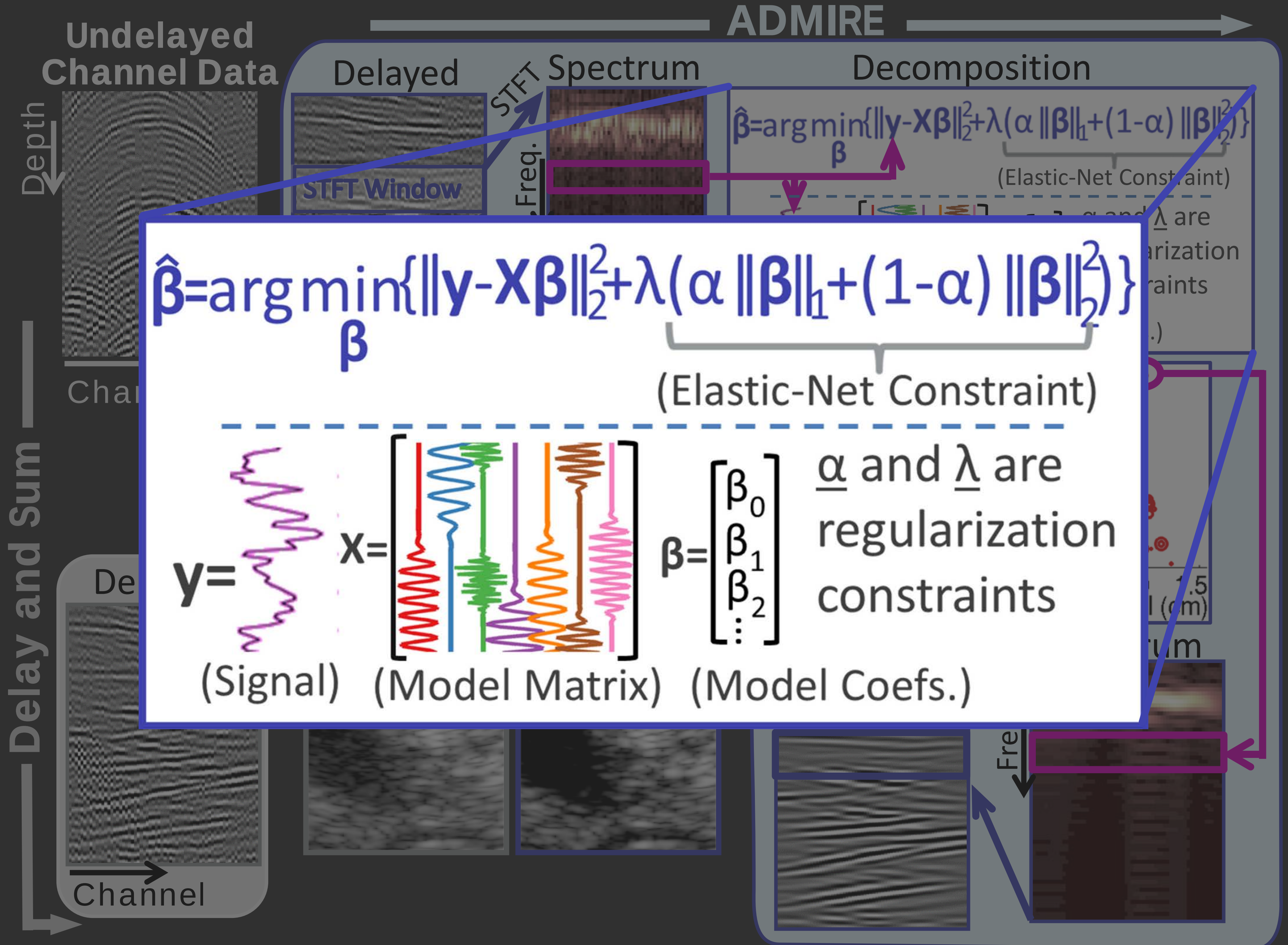

ADMIRE
Undelayed Channel Data
Depth
Delayed
STFT
Spectrum
Decomposition
STFT Window
Freq.
Delay and Sum
Channel
$\hat{\boldsymbol{\beta}} = \arg\min_{\boldsymbol{\beta}} \{ \|\mathbf{y} - \mathbf{X}\boldsymbol{\beta}\|_2^2 + \lambda(\alpha \|\boldsymbol{\beta}\|_1 + (1-\alpha) \|\boldsymbol{\beta}\|_2^2) \}$
(Elastic-Net Constraint)
y=
X=
$\boldsymbol{\beta} = [\beta_0, \beta_1, \beta_2, \vdots]$
α and λ are regularization constraints
(Signal)
(Model Matrix)
(Model Coefs.)

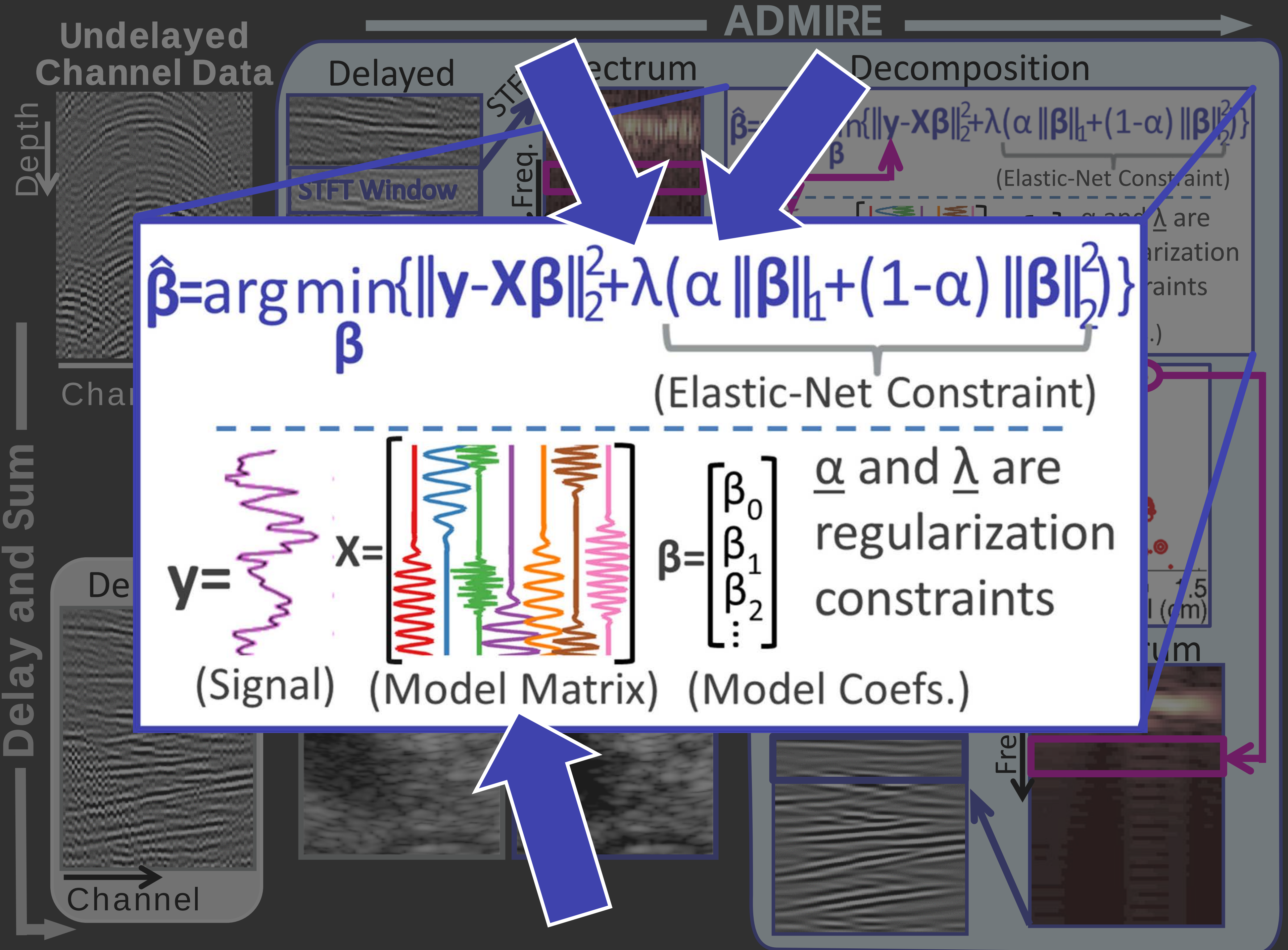
ADMIRE
Undelayed Channel Data
Depth
Channel
Delay and Sum
Delayed
STFT Window
STFT
Freq.
Decomposition
β̂=argmin{‖y-Xβ‖²₂+λ(α‖β‖₁+(1-α)‖β‖²₂)}
β
(Elastic-Net Constraint)
y=
X=
β=
β0 β1 β2 ⋮
α and λ are regularization constraints
(Signal)
(Model Matrix)
(Model Coefs.)
Channel

Linear Contrast Simulations ("All Pass Case")

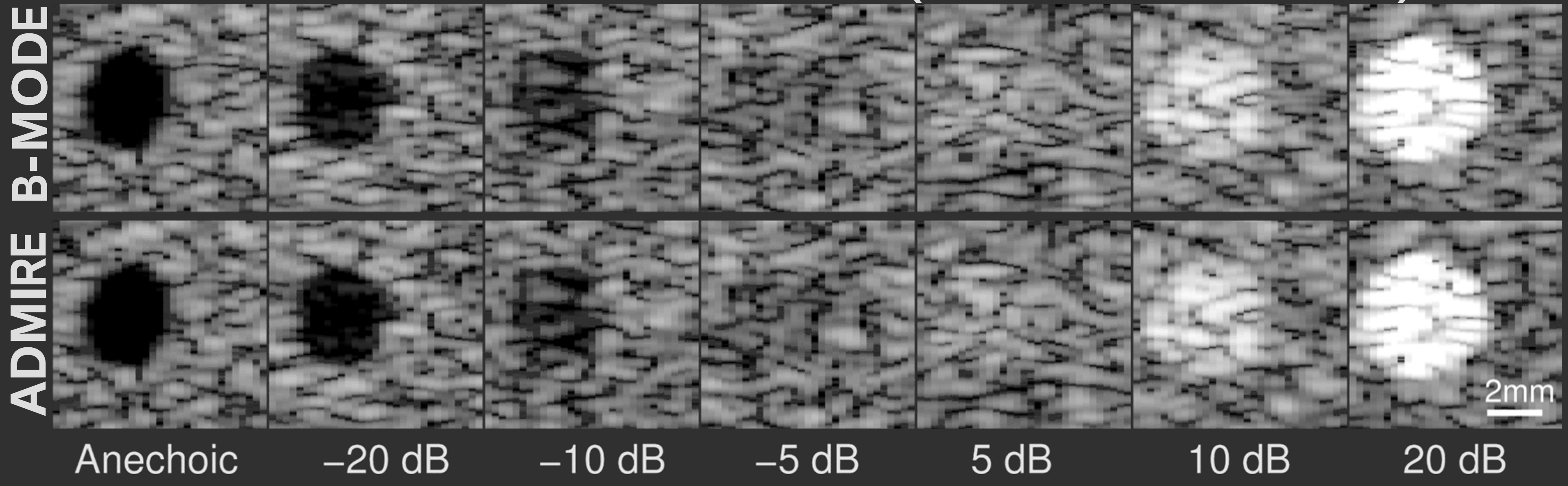

Contrast

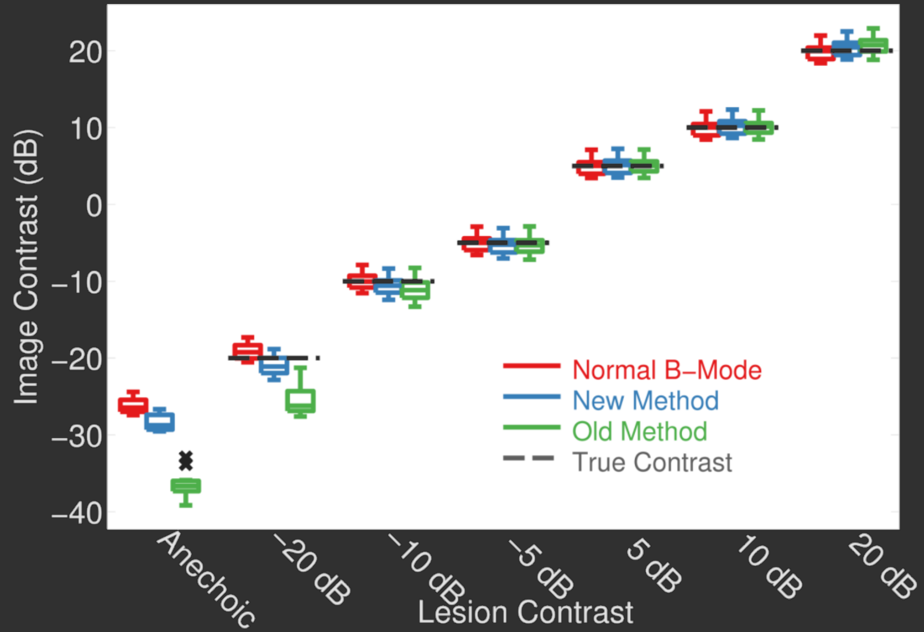

Contrast-to-Noise Ratio

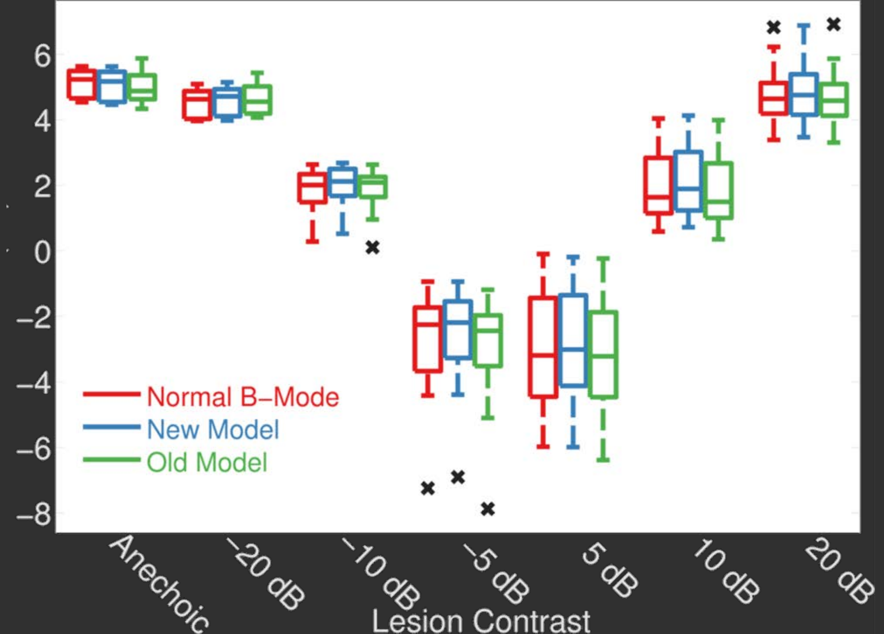

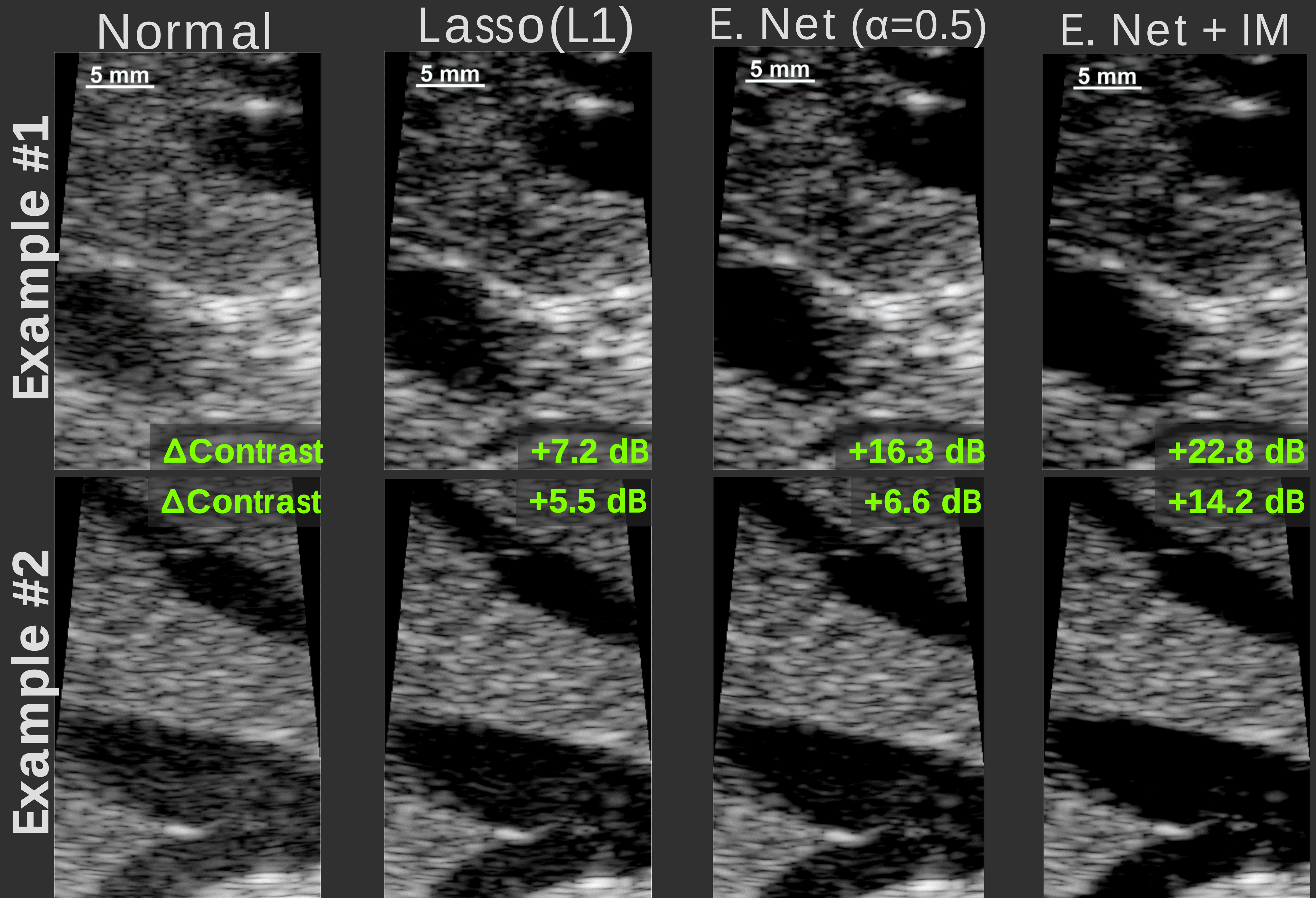

Normal
Lasso(L1)
E. Net (α=0.5)
E. Net + IM
Example #1
Example #2
5 mm
5 mm
5 mm
5 mm
ΔContrast
+7.2 dB
+16.3 dB
+22.8 dB
ΔContrast
+5.5 dB
+6.6 dB
+14.2 dB

Contrast

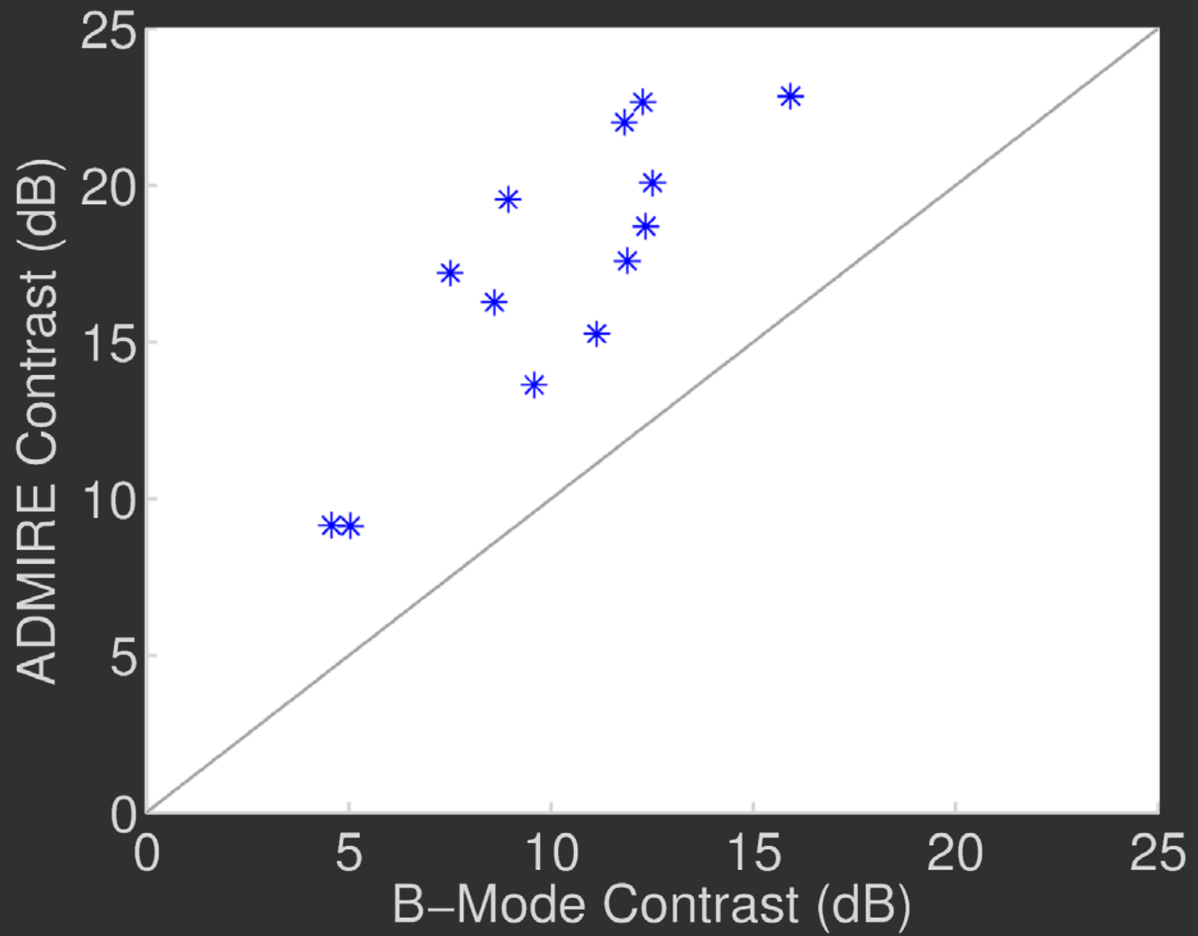

Contrast-to-Noise Ratio

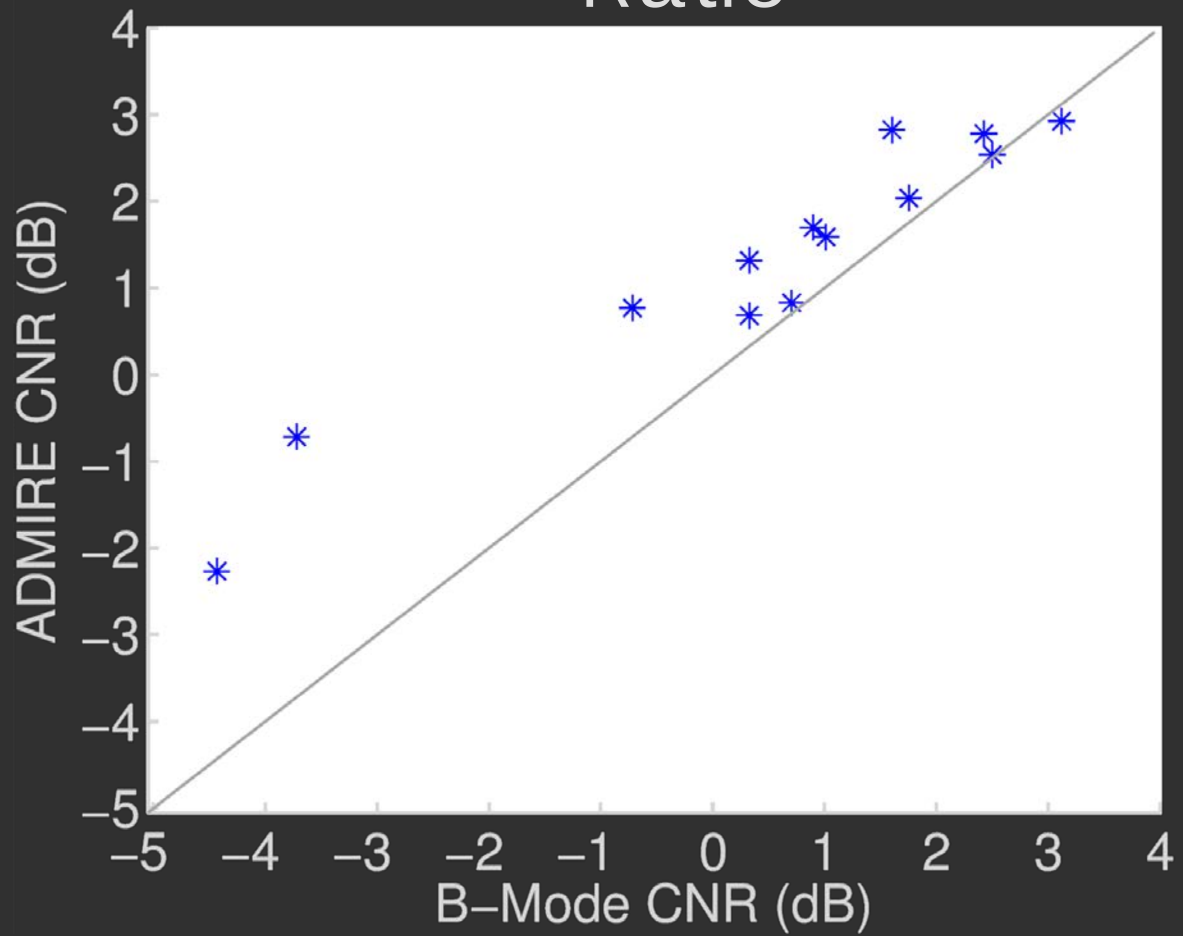

Improvement:

7.1±2.5 dB

0.86±0.92 dB

Second Harmonic Imaging

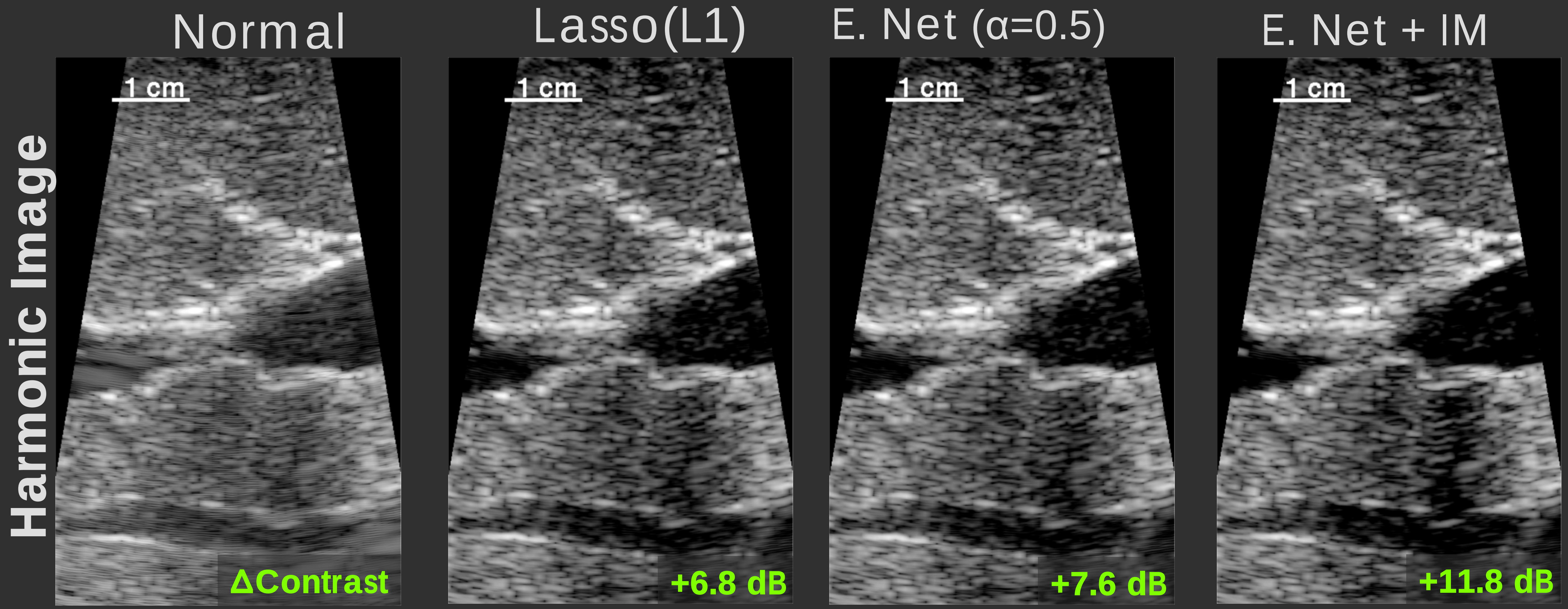

Harmonic Imaging

Contrast

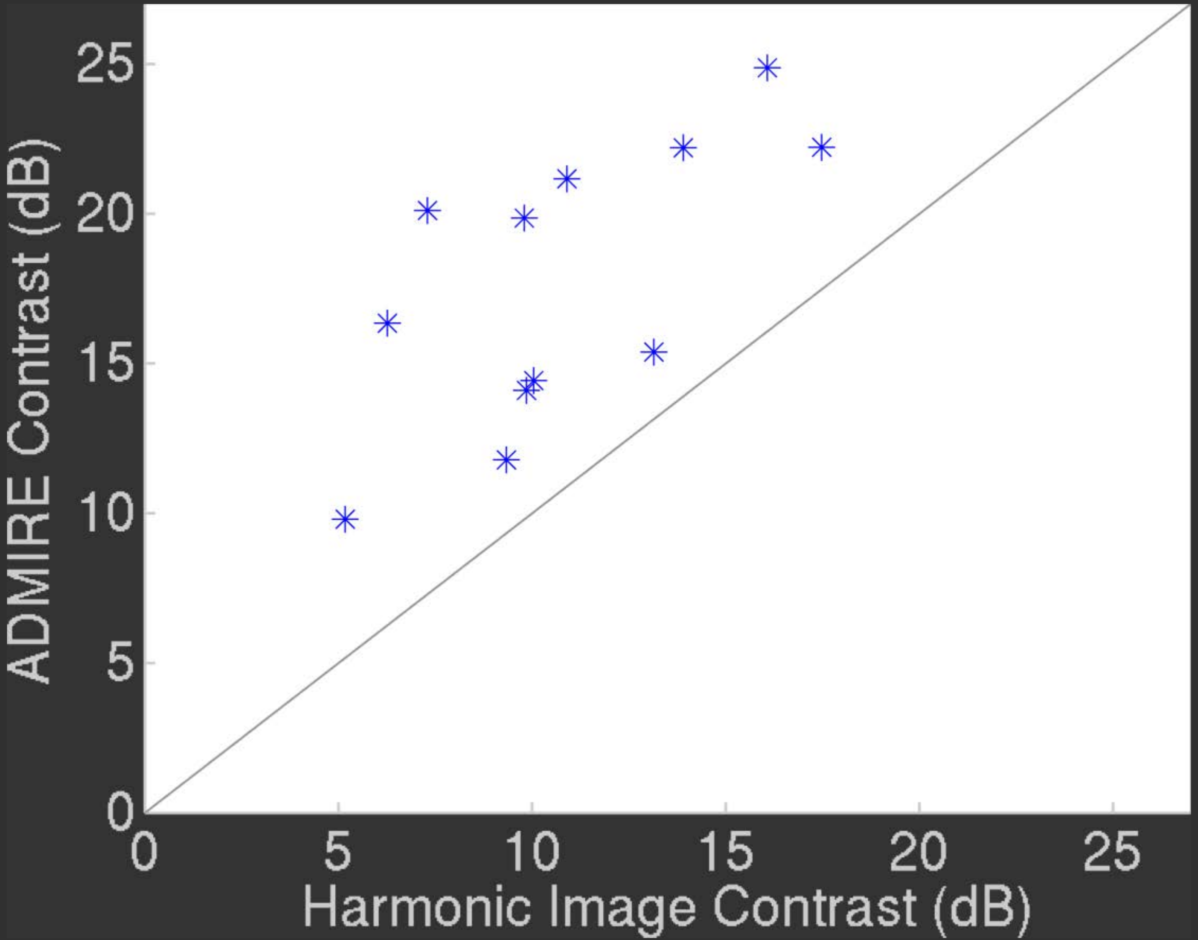

Contrast-to-Noise Ratio

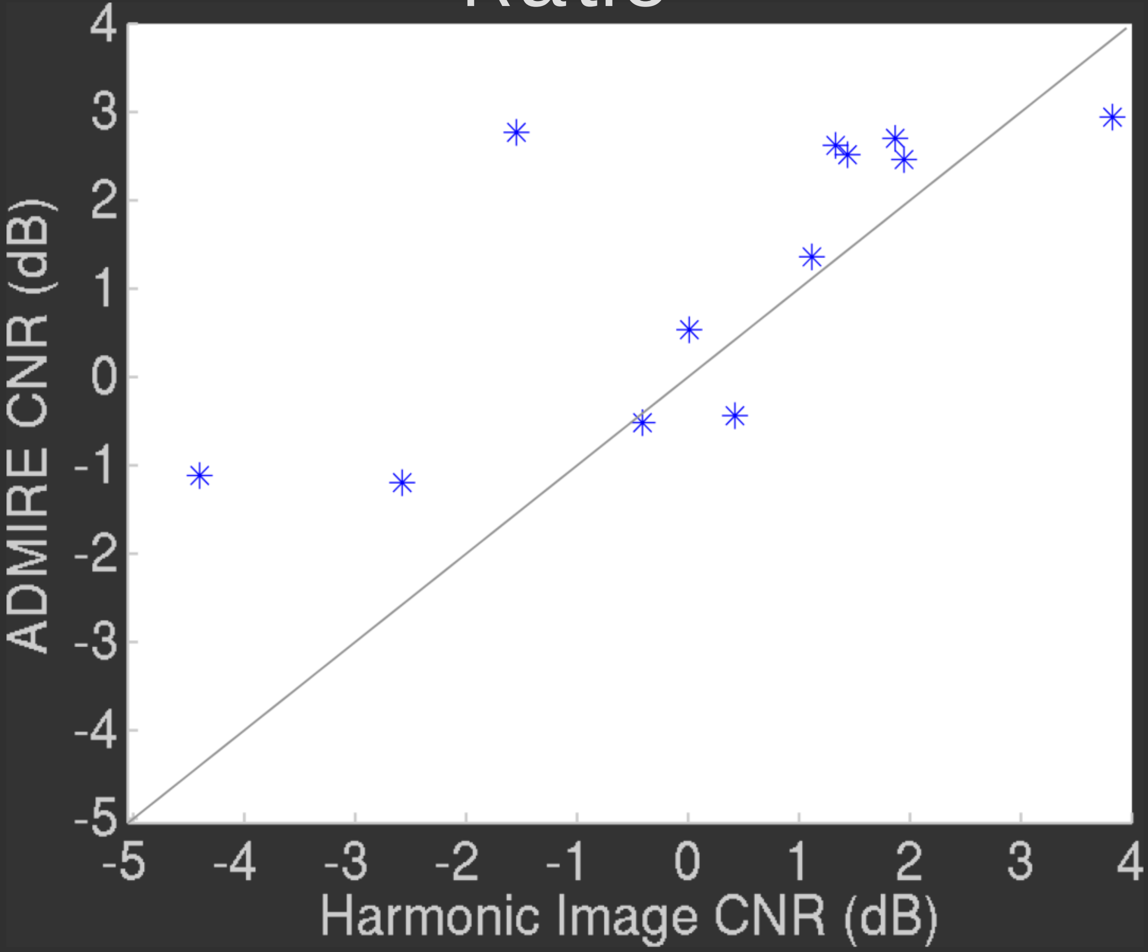

Improvement:

	Contrast	CNR
ADMIRE	6.9±3.5 dB	0.97±1.53 dB

Limitations of ADMIRE and other similar model-based strategies

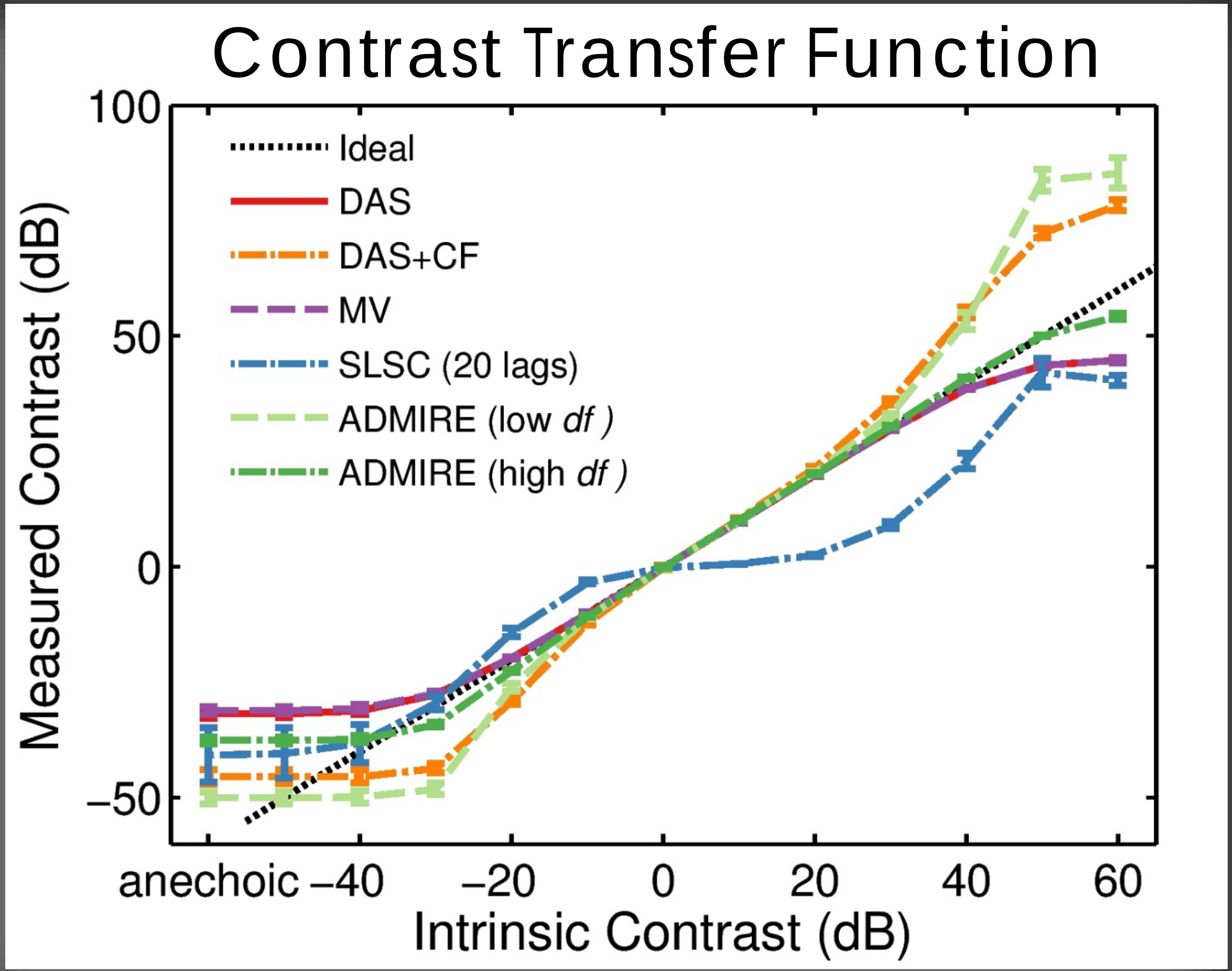

Beamformer	Dynamic Range
DAS	56.3 dB
DAS+CF	21.0 dB
MV	55.5 dB
SLSC	17.1 dB
ADMIRE (low, high *df*)	28.5 dB, **58.1** dB

Arbitrarily high contrast for anechoic cysts

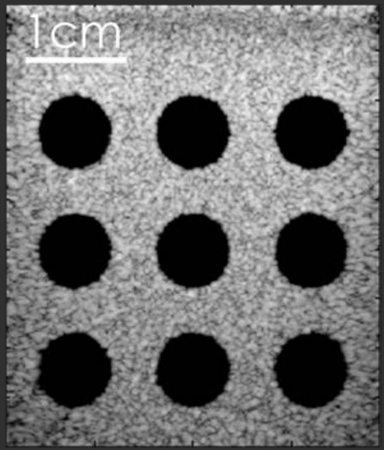

Dynamic Range Limitations

B-Mode

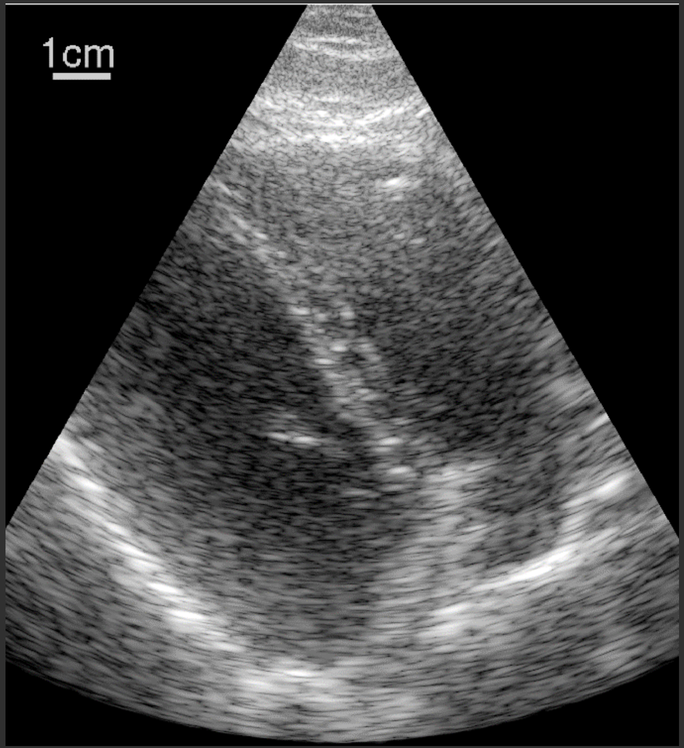

ADMIRE

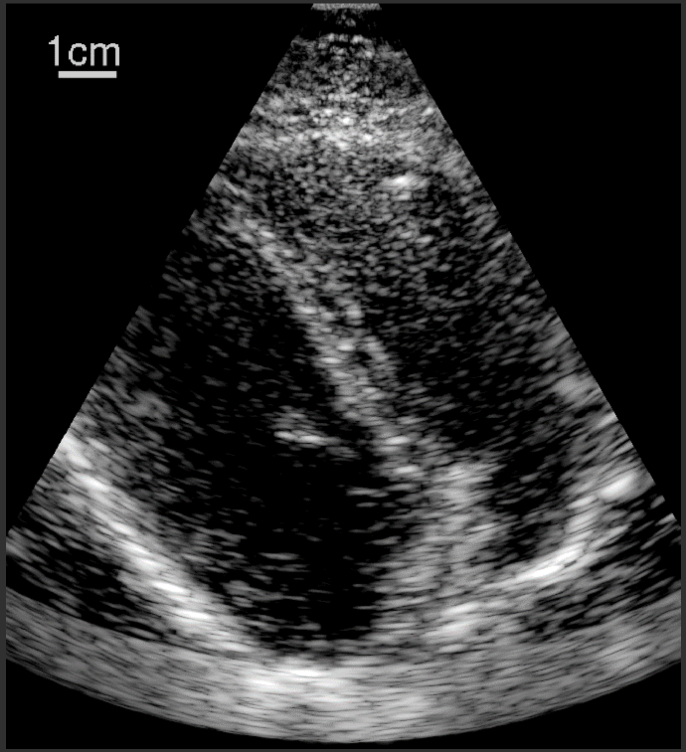

Regularization Schemes Fails at High Dynamic Ranges

B-Mode ADMIRE

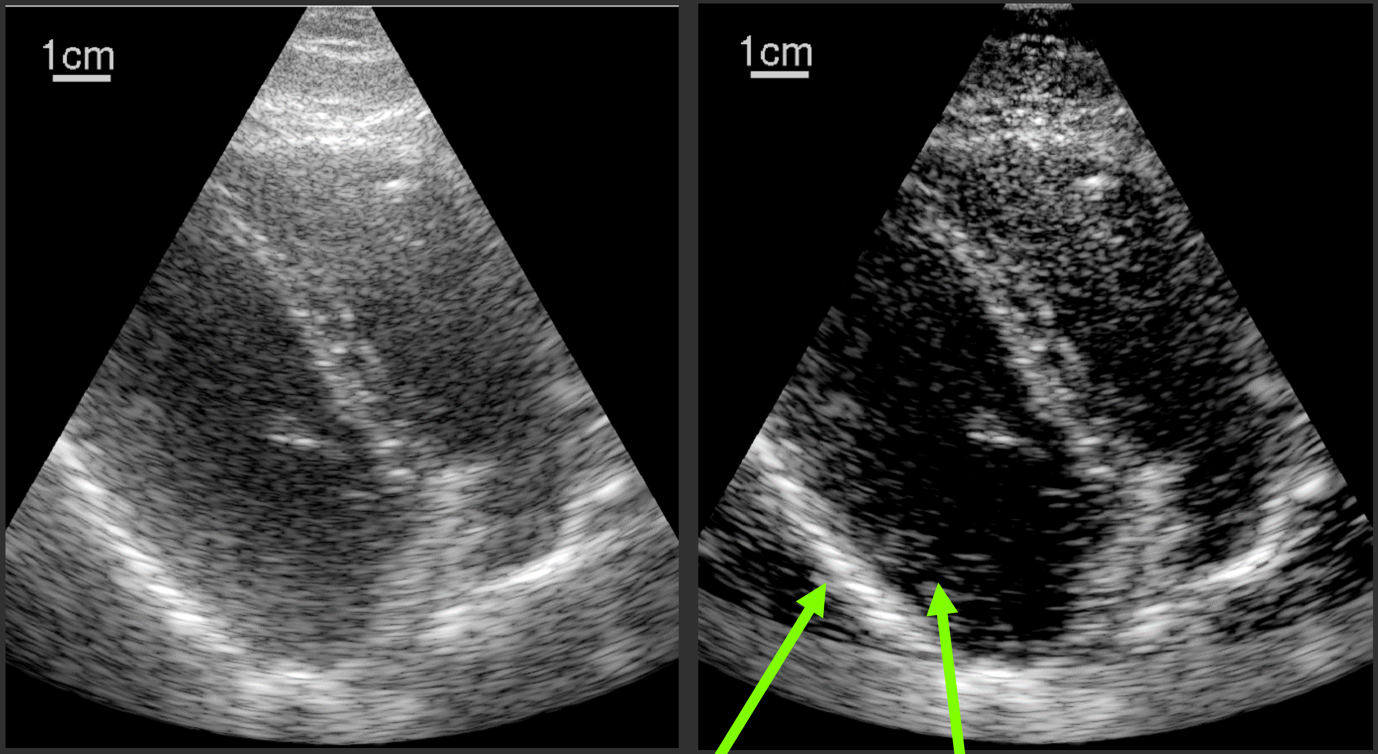

Bright scattering from pericardium and lung

Relatively muted scattering from myocardium

Regularization Schemes Fails at High Dynamic Ranges

B-Mode

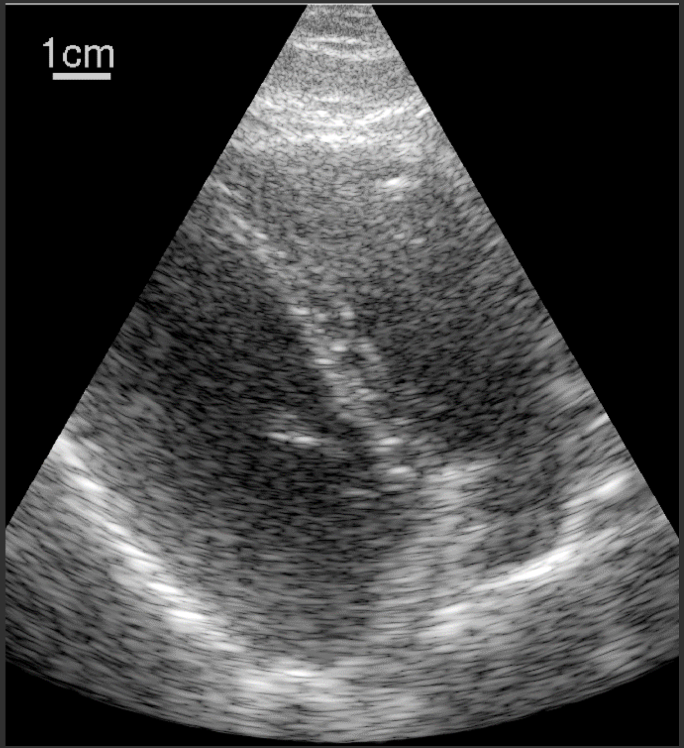

ADMIRE

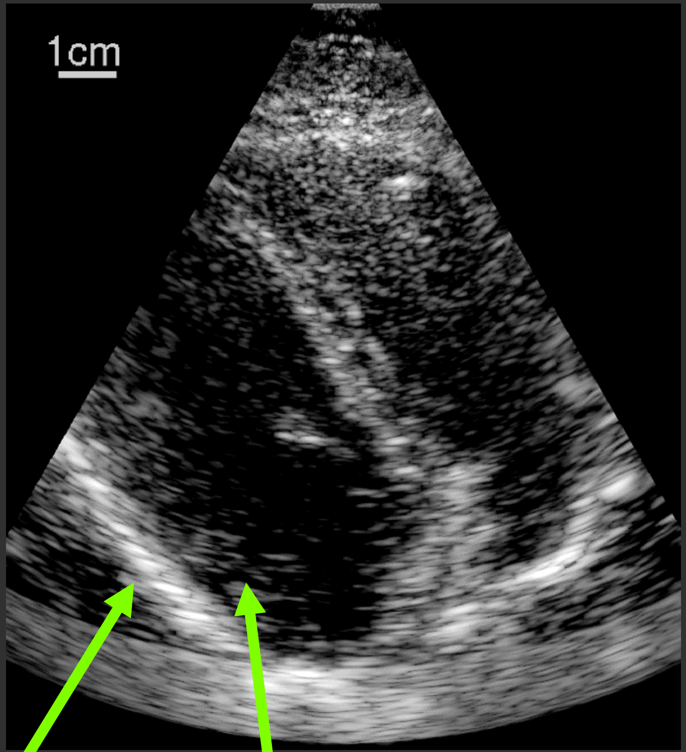

Some kind of constraint is required for the model fit, but the constraint limits the dynamic range

Bright scattering from pericardium and lung

Relatively muted scattering from myocardium

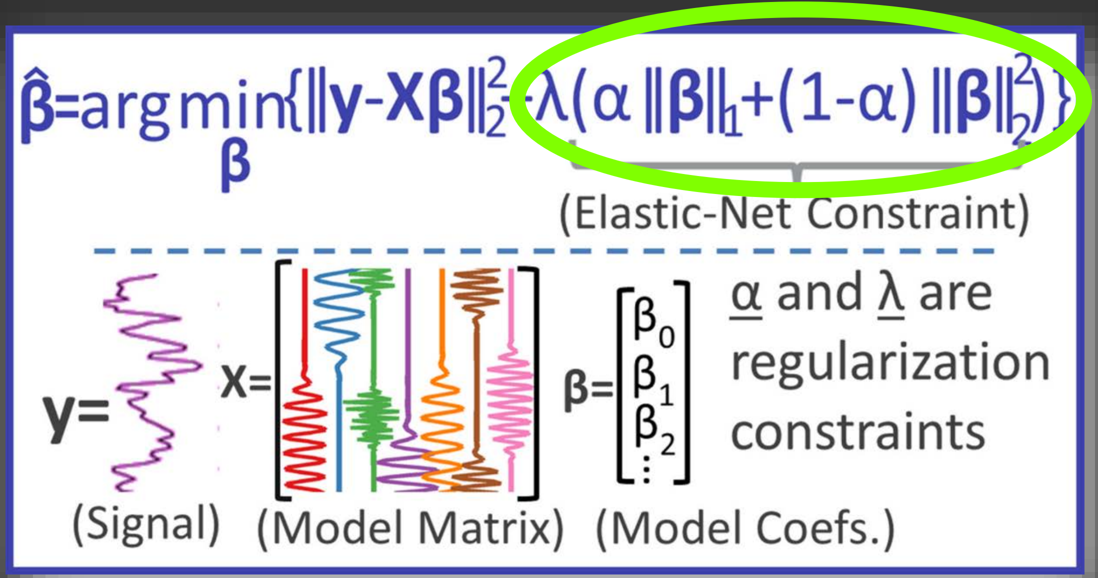

Regularization Schemes Fails at High Dynamic Ranges

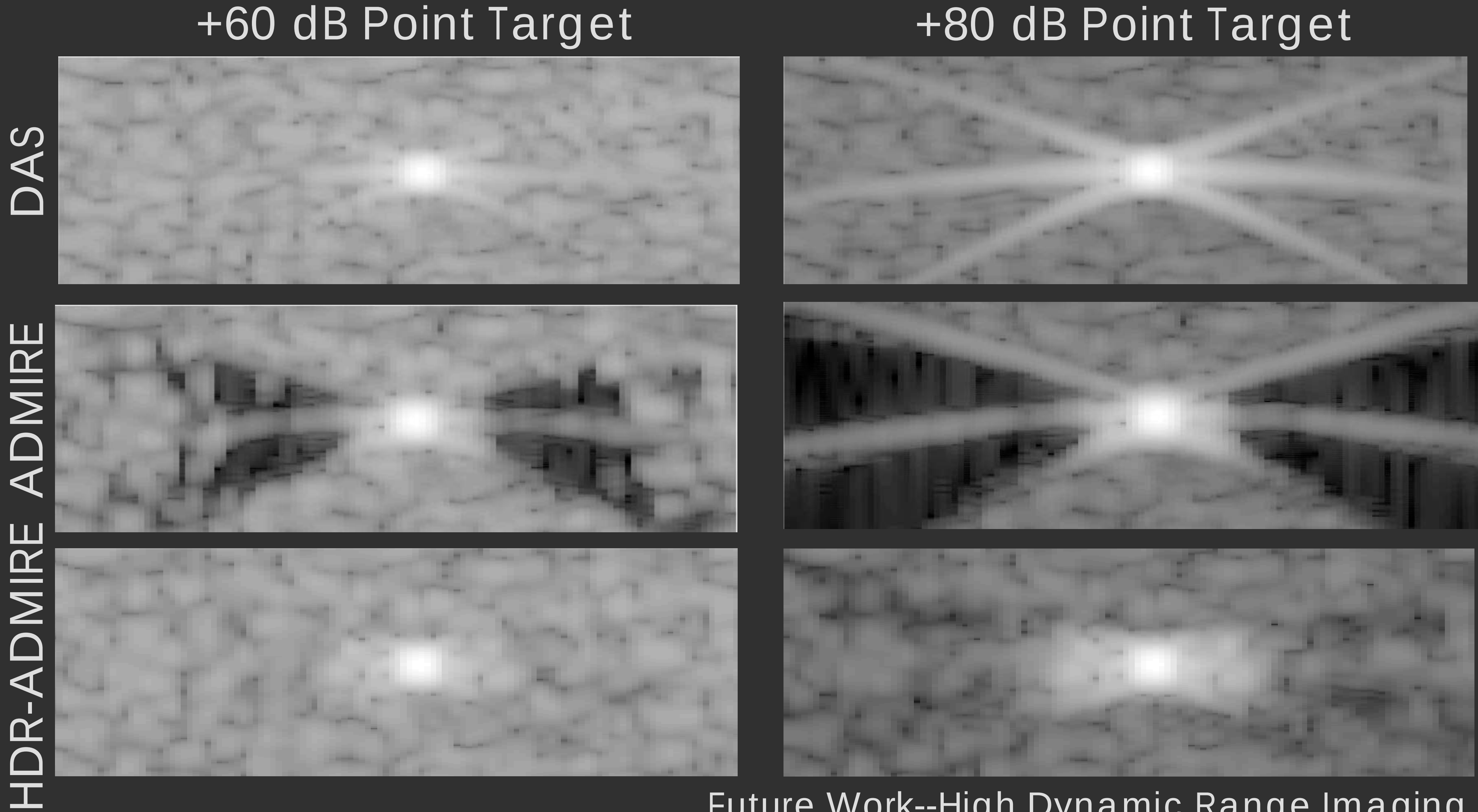

Future Work--High Dynamic Range Imaging

Model-based ultrasound image formation approaches offer many potential benefits

Evaluation of Model-based methods is easily gamed

Careful consideration of tuning can lead to improvements over DAS with few downslides

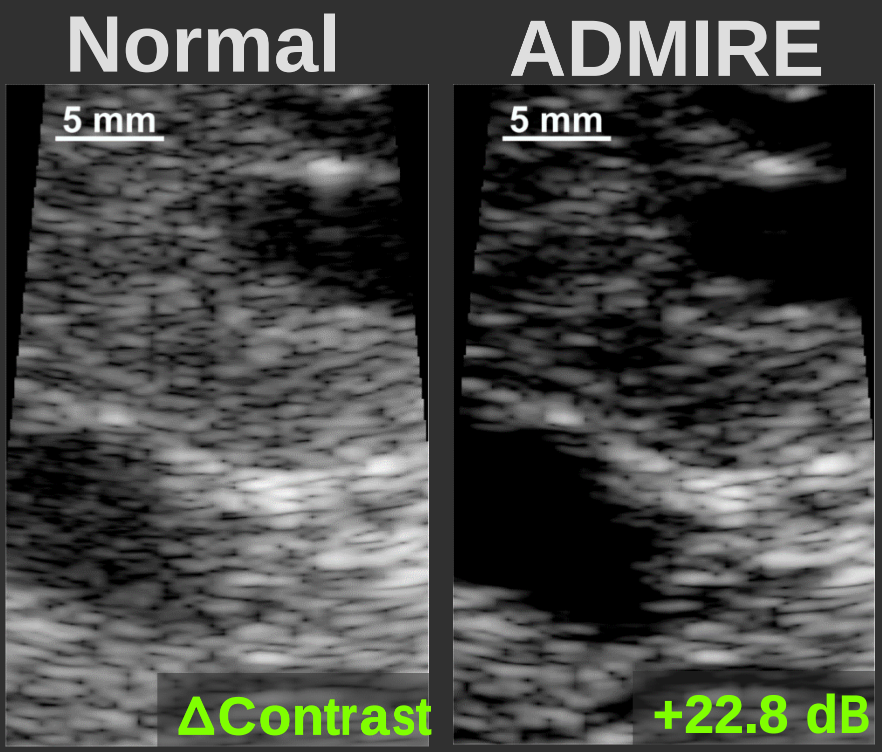

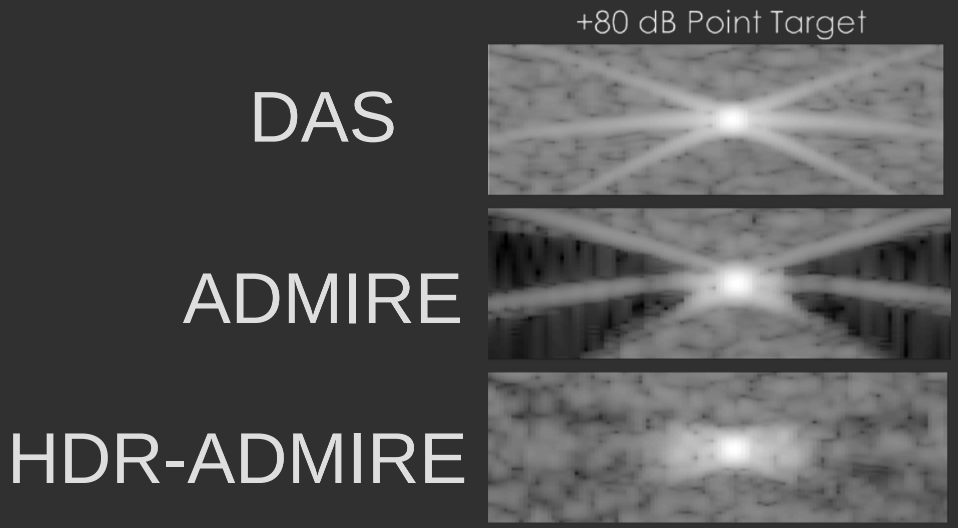

Conculsion

Collaborators:

Dan Brown

Michael Miga

Ryan Hsi

Ravindra Duddu

W. Dave Merryman

Other:

Douglas Dumont

Jeremy Dahl

Gregg Trahey

Kathy Nightingale

Kai Thomenius

Marko Jakovljevic

Nick Bottenus

Lab:

Adam Luchies

Kazuyuki “Kaz” Dei

Kristy Walsh

Jaime Tierney

Jasmine Shu

Katie Ozgun

Siegfried Schlunk

Funding:

NIH 1S10RR026828

NIH R01HL128715

NIH R01EB020040

Acknowledgements

Questions?